Engineering a Synthetic Dopamine-Responsive Riboswitch for *In Vitro* Biosensing

Svetlana V. Harbaugh,* Adam D. Silverman, Yaroslav G. Chushak, Kathryn Zimlich, Monica Wolfe, Walter Thavarajah, Michael C. Jewett, Julius B. Lucks, and Jorge L. Chávez

| ACCESS | | Metrics & More | | Article Recommendations | | Supporting Information |

ABSTRACT: The detection of chemicals using natural allosteric transcription factors is a powerful strategy for point-of-use molecular sensing, particularly using fieldable cell-free gene expression (CFE) systems. However, the reliance of detection schemes on characterized protein-based sensors limits the number of measurable analytes. One alternative solution to this issue is to develop new sensors by generating RNA aptamers against the target analyte and then incorporating them directly into a riboswitch scaffold for ligand-inducible genetic control of a reporter protein. However, this strategy has not generated more than a handful of successful portable cell-free molecular sensors. To address this gap, here we convert dopamine-binding aptamers into functional dopamine-sensing riboswitches that regulate gene expression in a freeze-dried CFE reaction. We then develop an assay for direct detection and semi-quantification of dopamine in human urine. We anticipate that this work will be broadly applicable for converting many *in vitro*-generated RNA aptamers into fieldable molecular diagnostics.

KEYWORDS: cell-free gene expression, TX-TL, biosensing, dopamine, human performance, riboswitch, aptamer
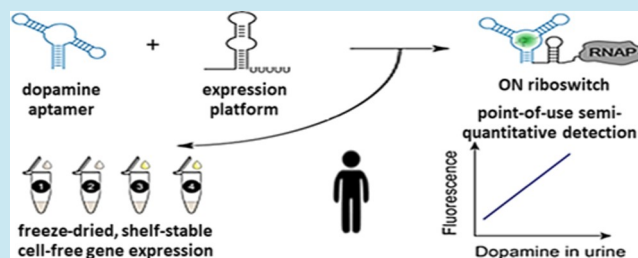
INTRODUCTION

Synthetic biologists have made great progress in harvesting natural sensing systems to engineer genetically encoded biosensors that can detect a wide variety of targets. Targets have included commodity chemicals and environmental contaminants such as explosives,[1,2] pesticides,[3,4] volatile organic solvents,[5,6] heavy metals,[7−10] viral or bacterial pathogens,[11,12] and biomarkers of human disease or nutritional state.[13,14] To detect such molecules, whole-cell biosensors (WCB), where genetically encoded biosensors incorporate an analyte-responsive protein that regulates the expression of a reporter gene in an engineered living cell, have been commonly used.[15,16] More recently, cell-free gene expression (CFE) has emerged as an alternative to WCBs for field-deployable molecular detection.[17] The low cost, ease of use, modularity, thermal stability, and limited biocontainment risk of freeze-dried CFE sensors have already demonstrated great promise for rapid, equipment-free detection of a wide array of chemicals[1,18−28] and nucleic acids.[29−34]

Molecular detection of chemicals using CFE canonically requires a transcription factor that responds to the target molecule—or a short catabolic pathway that can convert the target molecule to one that is detectable (i.e., "metabolic biosensing").[1,18,25] This constraint limits the availability of detectable targets. Synthetic riboswitches offer a possibility to expand the toolkit for the detection of new analytes. Riboswitches are RNA-based biosensing mechanisms that contain two domains: an aptamer that can bind a target ligand and a downstream expression platform that folds in different states depending on ligand binding to regulate gene expression. While natural riboswitches have been used in CFE-based systems to detect naturally abundant toxins,[35] there is great promise for engineering riboswitches to expand the range of detectable compounds.[36] In particular, systematic evolution of ligands by exponential enrichment (SELEX)[37] can be used to generate aptamers, which can then be incorporated into new riboswitches using RNA synthetic biology approaches. For instance, by creating a statistical thermodynamic model to map the relationships between riboswitch sequence, structure, and function, a library of synthetic switches was built from a range of aptamers to regulate translation initiation.[38] In another example, a "decoupled" expression platform from the natural *pbuE* riboswitch in *Bacillus subtilis* was modularly fused to synthetic aptamers against targets of interest to generate synthetic switches that regulate transcription.[39] Aptamers inserted into scaffolds of ribozymes can even be used as genetically encoded biosensors that are screened using next-
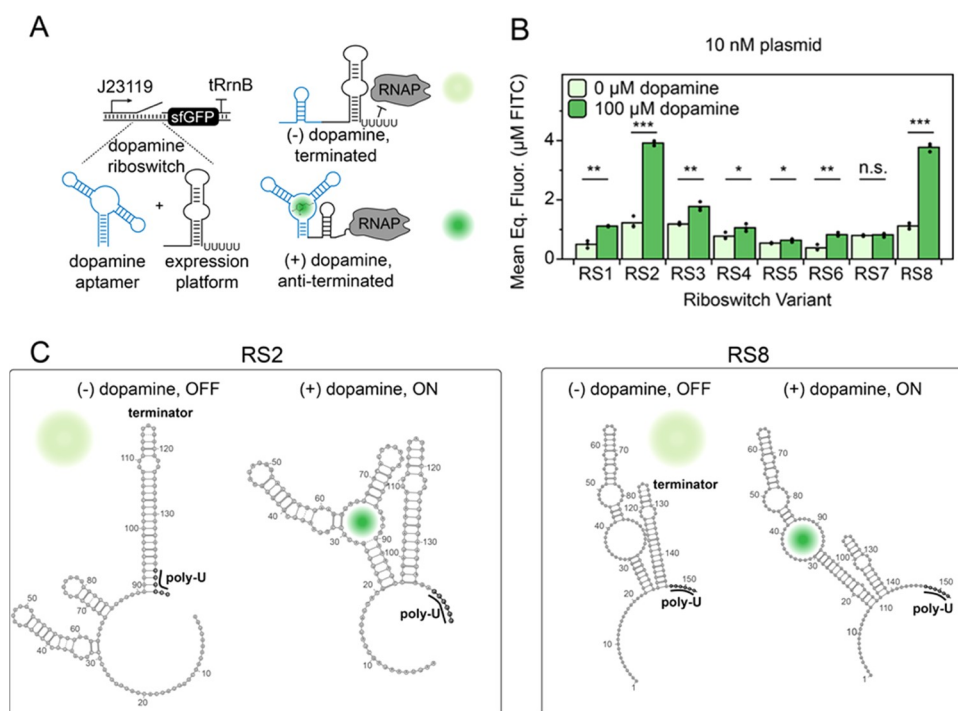
Figure 1. Design of a cell-free dopamine sensor. (A) Design and construction of dopamine riboswitches and deployment in a cell-free gene expression (CFE) platform. (B) sfGFP expression observed for a panel of riboswitch variants. Purified plasmid DNA (10 nM) corresponding to each designed riboswitch variant was added to a CFE reaction at a final concentration of 0 μM (OFF) or 100 μM (ON) dopamine. Reported endpoint values are the mean (bars) of three technical replicates (displayed as individual data points) after 4 h at 30 °C, background-subtracted by a no-DNA blank. Statistical comparisons between ON and OFF conditions: * indicates $p < 0.05$, ** indicates $p < 0.01$, and *** indicates $p < 0.001$, from one-tailed Student's t-test, assuming unequal variances from $N = 3$ points. (C) Schematic representation of RS2 and RS8 riboswitch folds modeled from the full-length RNA sequence using Mfold.[48] Without dopamine, the expression platform is predicted to fold into an intrinsic terminator (nucleotides 89−141 in RS2 and 104−146 in RS8), ending in a poly-uracil tract. Dopamine binding to the aptamer was modeled by constraining aptamer secondary structure to prevent the formation of the terminator, activating the expression of the downstream gene. Secondary structures were rendered using VARNA and modified in Adobe Illustrator for clarity.[49]

generation sequencing.[40,41] When coupled to laboratory-based aptamer evolution approaches, any of these strategies could provide a tool to rapidly design, build, and test novel sensors for targets of interest, ideally active in a CFE platform that is compatible with point-of-use molecular diagnostics.

In practice, though, there are still several important challenges to be addressed in the field of *de novo* riboswitch engineering. Many existing synthetic riboswitches rely on a relatively small set of compatible and modular aptamers for targets that have little environmental or health relevance (e.g., theophylline, tetracycline, and various nucleotide and nucleotide derivatives[42]). Additionally, most engineered riboswitches lack the sensitivity and specificity required for real-world diagnostic applications. The only riboswitch so far deployed in a practical CFE diagnostic context to date is the natural fluoride-sensing *crcB* element from *Bacillus cereus*.[35] Ideally, new switches could be constructed from synthetic aptamers to bind to heavy metals, organic chemicals, or diagnostic metabolites, filling in the gap for the detection of molecules with no known natural sensors.

As a proof of concept for the *de novo* design of riboswitches for CFE, we considered dopamine, a biomarker of human performance and health and an ideal target, to test our approach to sensor development for several reasons. First, although several dopamine aptamers have been developed and characterized,[36,43] including one that was integrated into a translation-regulating riboswitch with a modest (∼2×-fold) activation ratio,[38] no synthetic dopamine riboswitches have so far been reported to regulate transcription. We considered the available structural and sequence diversity of dopamine-sensing aptamers to be a benefit, since constructing riboswitches out of diverse structures would validate the modularity of the approach. Second, dopamine is a compelling detection target for a point-of-use biosensor. Both elevated and depressed levels of dopamine are indicative of stress or human disease.[44,45] Because dopamine concentrations oscillate over the course of the day in different sampled body fluids,[46] simple noninvasive and semi-quantitative dopamine monitoring[47] could be particularly useful for monitoring human health status.

Here, we demonstrate a workflow for designing a synthetic transcriptional riboswitch for *in vitro* point-of-use detection of dopamine. We screen a variety of characterized dopamine aptamers inserted into the scaffold of a transcriptional riboswitch and find two variants that efficiently regulate CFE in response to dopamine, with a small amount of cross-reactivity to other catecholamines. We then provide a proof of concept for cell-free dopamine sensing using the riboswitch in diluted human urine, a complex and clinically relevant sample matrix. We develop a strategy for semi-quantification of analyte concentration that relies on the linearity of both the riboswitch dose−response curve and matrix poisoning effects. We envision that the strategies reported here could be directly extended to develop other synthetic riboswitches for use in cell-free molecular detection.
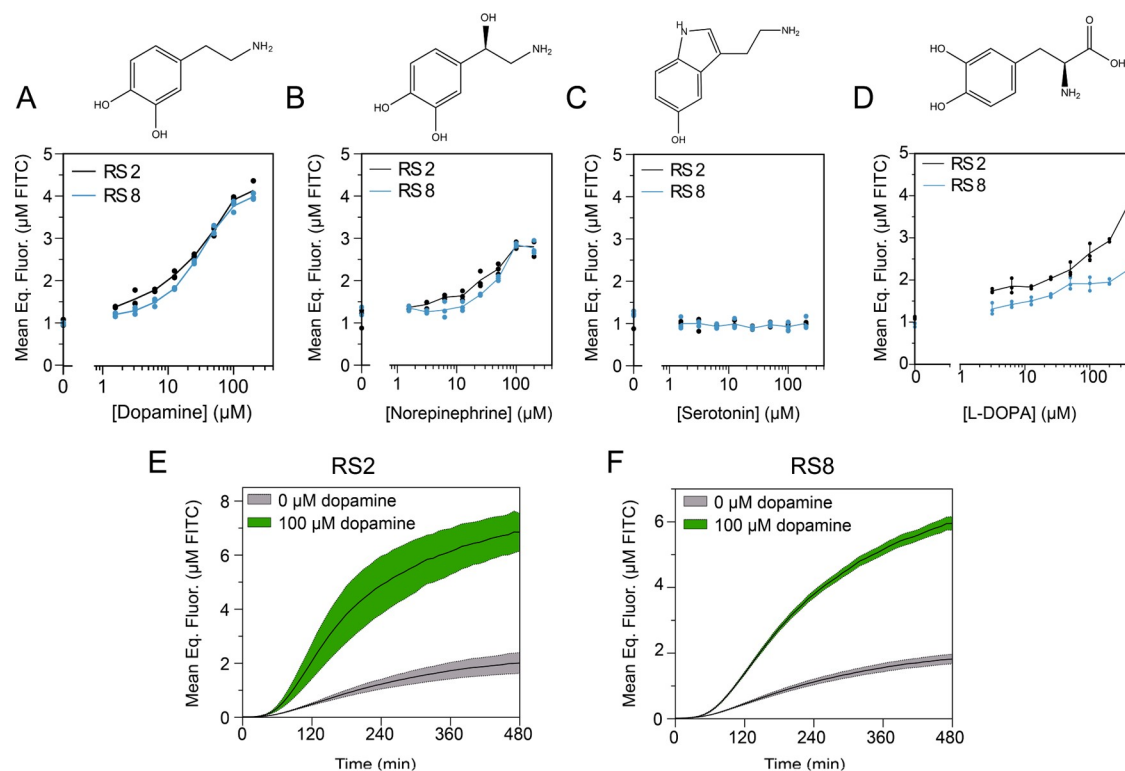
Figure 2. (A−D) Analyte titration for other competing ligands for functional riboswitch variants; 10 nM of each riboswitch reporter plasmid was incubated in separate reactions with the indicated ligand at log-fold increments. Final sfGFP concentrations are reported after 4 h at 30 °C. Points indicate individual replicates ($N = 3$) after background-subtraction and calibration to a FITC standard curve. (E, F) Kinetics of activation of RS2 and RS8. Reported are the sfGFP concentrations normalized to a FITC standard over an 8-h CFE experiment at 30 °C, supplied with 10 nM of the respective plasmid and either 0 or 100 μM dopamine, and continuously monitored every 10 min for RS2 (E) and RS8 (F). Shaded areas represent the mean of $N = 6$ measurements, ± 1 standard deviation.

RESULTS

Design of Dopamine-Responsive Riboswitches as Cell-Free Biosensors. To build transcriptional dopamine riboswitches, we selected eight dopamine RNA aptamers previously generated from two different SELEX strategies (see the Supporting Information, Table S1 for the aptamer sequences). Mannironi et al.[43] used SELEX to find RNA aptamers that specifically bound to a dopamine-agarose column, starting from a randomized N80 library of 3.4 × 10^14 sequences. In the work from the Batey lab, dopamine-binding RNAs were selected by mutating the three-way junction aptamer scaffolds from natural riboswitches.[36] We chose dopamine aptamers from each study and directly fused them to the expression platform of the reengineered *B. subtilis* *pbuE* riboswitch (*pbuE/pbuE**), as previously described.[39] The expression platform consists of a pre-aptamer sequence and a post-aptamer sequence harboring a rho-independent transcription terminator with six uridine residues on the 3′-side, where transcription terminates (Supporting Information, Table S1). Previously, it was demonstrated that reducing the number of uridine residues from eight to six in the poly-uridine tract on the 3′-side of the terminator in *pbuE/pbuE** riboswitch reduces termination efficiency and results in a greatly improved riboswitch response.[39] To conveniently measure gene expression in the presence and absence of dopamine in a CFE reaction, we cloned these riboswitch variants (RS) between the synthetic *Escherichia coli* promoter J23119 and the coding sequence of superfolder green fluorescent protein (sfGFP), including a common upstream ribosome-binding site (RBS).

(Figure 1A). Because the riboswitch and reporter are encoded in *cis*, and there are no accessory protein factors, sensor tuning is particularly simple. The riboswitch sensor plasmids were added to CFE reactions to a final concentration of 10 nM in the presence or absence of 100 μM dopamine. We then measured the fluorescence of the reactions after 4 h at 30 °C on a plate reader and correlated the readings to a linear calibration curve obtained for titrations of fluorescein isothiocyanate (FITC), a traceable chemical standard (Figure 1B).

Of the eight switches that we constructed, seven showed a statistically significant ($p < 0.05$) increase in the final sfGFP produced when dopamine was added. However, most showed only modest fold-activation between 1 and 2 when comparing presence (ON) versus absence (OFF) of dopamine. Only two variants, RS2 and RS8, displayed fold-activation greater than 3, mainly because these had the highest ON states among all of the sensors. Using an RNA structure prediction tool, we characterized the folding of these two riboswitches in the putative OFF and ON states (Figure 1C). Interestingly, we did not observe any trends in the experimental binding affinity of the aptamers (Supporting Information, Table S2) or the thermodynamics or kinetics of folding that would explain why RS2 and RS8 switched better than the other six riboswitches screened (Supporting Information, Table S3). To monitor the kinetics of transcription and validate that the switches regulated protein synthesis at the level of transcription, we fused a malachite green RNA aptamer to the 3′ end of the sfGFP reporter to simultaneously measure transcription and translation rates in orthogonal fluorescence channels.[50] As
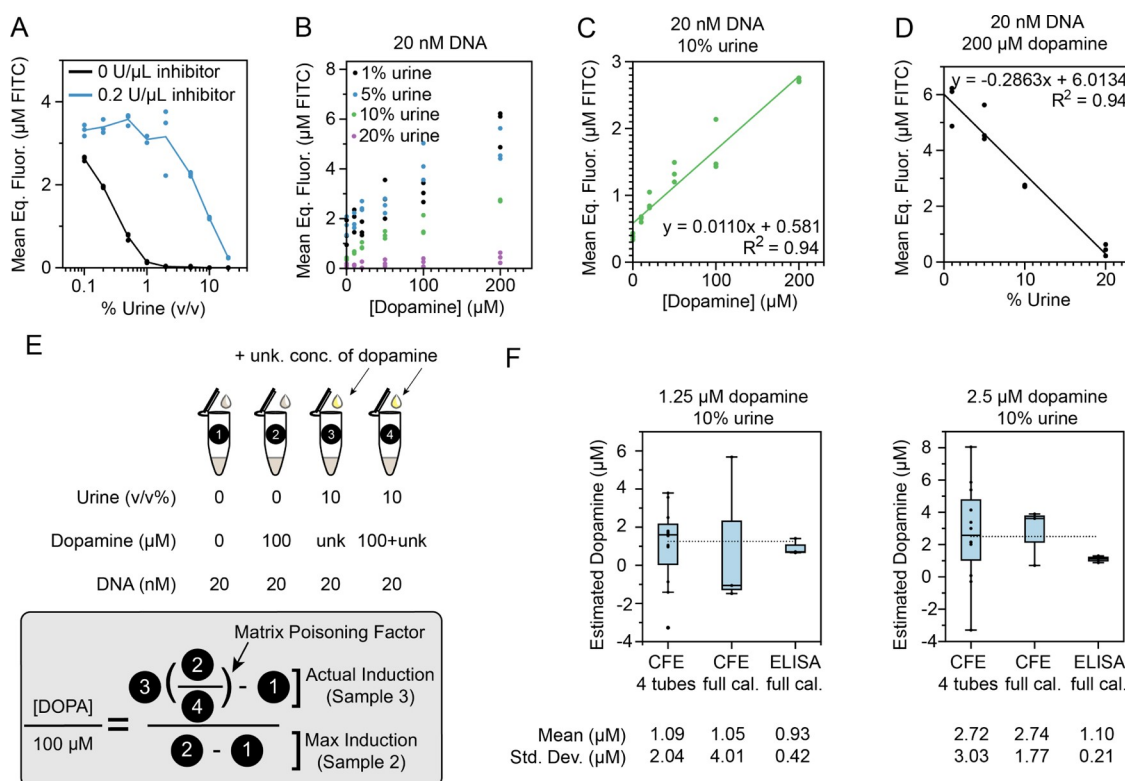
Figure 3. Semi-quantification of dopamine in human urine sample matrix. (A) Pooled human urine poisons CFE of constitutively expressed sfGFP at volume fractions above 1%. Supplementation of 0.2 U/μL murine RNase inhibitor rescues expression up to approximately 10% urine v/v. Construct pJBL7010 was included at 20 nM to express sfGFP. (B) Cell-free dopamine dose−response curves for 20 nM RS2 riboswitch variant plasmid as a function of urine concentration. (C) Most linear dose−response curve for dopamine occurs with 20 nM reporter DNA and 10% urine v/v, indicating this condition is optimal for quantification efforts. (D) Urine poisoning response curve is also linear when the dopamine and DNA concentrations are fully saturating. Note that additional dose−response curves are provided in the Supporting Information, Figures S4 and S5. We chose 100 μM dopamine as the final concentration to ensure the dopamine induction remains in a linear operating range when reporter expression is high. (E) Quantification scheme for cell-free dopamine detection in a urine matrix. The ratio between tubes 2 and 4 can be used to quantify the effect of matrix poisoning from urine, which is used to back-calculate the impact of urine and the impact of dopamine in unknown sample 3. (F) Comparison of quantification of low dopamine concentration in 10% of either the four-tube lyophilized cell-free expression assay, interpolation from a full cell-free dose−response curve, or measurement by a commercial dopamine immunoassay. The horizontal line indicates the true spiked dopamine concentration; bars represent the average of three independent technical replicates of sample conditions; and dots represent the individual measurements. All cell-free experiments were run from lyophilized reactions, rehydrated with the indicated urine concentrations spiked with fresh dopamine, and measured by a plate reader at 30 °C for 4 h. The four-tube experiments were done with N = 12 technical replicates; the full calibration curve and enzyme-linked immunosorbent assay (ELISA) were run with N = 3 technical replicates.

expected, transcription through RS2 and RS8 increased in the presence of dopamine, and levels of synthesized transcripts correlated with levels of produced sfGFP for all riboswitches (Supporting Information, Figure S1).

We next further characterized these two riboswitches for their utility in molecular sensing. First, to compare the ON signals, we titrated the reporter plasmids in the presence of dopamine and found that each variant could generate up to 6 μM FITC equivalent of sfGFP when 20 nM plasmid DNA was supplied to the CFE reaction (Supporting Information, Figure S2). At even higher DNA concentrations, we observed some decrease in expression, though we anticipate this is likely due to either a trace contaminant in the plasmid stock or due to a misallocation of transcriptional and translational resources, as has been previously reported.[51] Next, we characterized the sensing ability of each switch. Sensitivity and specificity are important for any molecular biosensor but particularly for riboswitches, which tend to bind less tightly[52] and less cooperatively[53] to small molecules compared to proteins. To quantify these effects, we titrated dopamine as well as three chemically related compounds (norepinephrine, serotonin, and

L-DOPA) into reactions containing 10 nM of each of RS2 and RS8 riboswitch plasmids (Figure 2A−D). The response functions and kinetics of activation (Figure 2E,F) for both riboswitch variants were generally similar, even though these aptamers vary greatly in sequence and structure and were derived from wholly independent selections. In each case, the estimated limit of detection for dopamine was sub-micromolar (LoD = 0.48 μM for RS2 and 0.96 μM for RS8), and the operating range was linear between 1 and 100 μM. Norepinephrine was similarly detected but with less sensitivity (LoD = 15 μM for RS2 and 18 μM for RS8) by both sensors, and neither switch responded to serotonin. Indeed, the only major functional difference we observed between RS2 and RS8 was in their responses to L-DOPA. RS2 was, in fact, initially evolved by SELEX to bind to L-DOPA and so predictably senses it much better than RS8, which was only evolved for dopamine binding. With a slightly better limit of detection and speed of response, we chose RS2 as the variant to carry forward for further development.

Efforts for Semi-Quantification of Dopamine in a Complex Sample Matrix. We next sought to establish a cell-

free dopamine sensor for semi-quantitative molecular diagnostics, aiming to develop an easy-to-use tool to indicate elevated levels of a stress biomarker on-demand outside a laboratory. Among common human biological sample fluids (saliva, whole blood, serum, sweat, urine), the concentration of dopamine is highest in human urine, with concentrations typically in the range of 100−500 ppb ($\sim$1−5 μM).[46] Fortunately, this physiological range matches fairly closely with the limit of detection we found from RS2 (Figure 2A), which suggests that the riboswitch is already properly tuned, and because the concentration of norepinephrine in urine is around one order of magnitude lower than dopamine,[54] crosstalk due to riboswitch promiscuity is unlikely.

However, undiluted urine poisons CFE reactions, likely because it contains additional nucleases, proteases, and salts that inhibit in vitro transcription and translation. Previous work has shown that supplementing RNase inhibitors can rescue some cell-free sensor activity.[25,55,56] We found that murine RNase inhibitor by itself could rescue constitutive protein synthesis for freeze-dried CFE reactions rehydrated up to approximately 20% urine by volume, but higher urine and salt[57] concentrations were not well-tolerated (Figure 3A, Supporting Information, Figure S3). Boiling the urine or passing it through a filter recovers even higher expression from the reactions rehydrated with 10% urine, likely by inactivating both RNases and proteases. However, we decided against relying on these strategies because they require additional equipment and time and could potentially distort the effective concentration of dopamine in the sample (Supporting Information, Figure S4).

These matrix effects add two complications to our diagnostic efforts. First, although the cell-free sensor may still detect high concentrations of dopamine spiked into the diluted urine samples, the 5× dilution factor necessary to eliminate the worst sample matrix poisoning effectively desensitizes the sensor so that it can no longer detect dopamine in a physiological range. Second, sample matrix effects complicate analyte quantification. We measured the freeze-dried cell-free sensor's dose–response to dopamine in the presence of four different urine ratios and found that all signals were depressed as urine concentration increased, as expected (Figure 3B). However, given just a single low fluorescence measurement, it would be difficult to ascertain if the signal was low because of a high concentration of urine or a low concentration of dopamine. This issue is compounded by substantial expected variability in the concentration of matrix inhibitors from donors of different hydration states. We therefore sought to design a simple scheme to calibrate against matrix effects from our sensor by measuring, side-by-side, control tubes that are insensitive to dopamine to solely represent the impact of urine inhibition. Our strategy builds on a previously published scheme for a colorimetric cell-free sensor that measured zinc in human serum semi-quantitatively by measuring the matrix poisoning in a reaction freeze-dried with a saturating concentration of analyte.[21]

Our strategy relies on the fact that both urine inhibition and dopamine induction are relatively linear across our target operating range (Figure 3B−D). Choosing reaction conditions that provide high, stable linearity and dynamic range for both dopamine dose–response and urine matrix poisoning (20 nM DNA, 10% urine by volume, and 100 μM dopamine, Supporting Information, Figures S5−S7), we devised a simple formula that would adjust for the matrix poisoning effect by

dividing the sample tube's fluorescence by a linear "poisoning factor" measured on the dopamine-saturated controls (Figure 3E). Ideally, this strategy would allow us to avoid constructing a full calibration curve for each new sample matrix, as was required for previous quantification approaches, which would greatly simplify the assay and reduce the cost, particularly if it is run in parallel on many samples with distinct inhibition profiles.[21] In a simple proof-of-concept experiment, our scheme to remove the effect of linear matrix poisoning allowed us to estimate low (1−3 μM) concentrations of dopamine spiked into a dilute urine sample matrix with similar accuracy to a complete calibration curve developed for the same sample, and with better accuracy than a commercial enzyme-linked immunosorbent assay (ELISA) kit calibrated in a 10% urine matrix (Figure 3F, Supporting Information, Figure S8). It should be noted that we were unable to determine the presence of dopamine in nonspiked urine samples using a commercial ELISA kit, so we assumed that it was 0 μM. Although our predictions of dopamine concentration are still of relatively low confidence due to high experimental error and substantial background signal, these challenges equally hinder confidence in the immunoassay, which is more complicated, expensive, and requires more hands-on time to run (Supporting Information, Figure S9). Overall, we found that the cell-free expression scheme gave us a more accurate measurement of dopamine spiked into urine samples than did the ELISA, albeit with greater variability.

■ DISCUSSION

Riboswitches derived from evolved aptamers are an appealing means for synthetic ligand-inducible gene expression, particularly as biosensing elements for diagnostics. In this work, we demonstrate that two independent synthetic dopamine-sensing aptamers could be incorporated into a natural riboswitch expression platform to generate a switch that regulates transcription in a lyophilized cell-free diagnostic at physiological concentrations of dopamine. We then provide a set of proof-of-concept experiments to justify this sensor as a diagnostic tool, even in the presence of inhibitory sample matrix effects. In tandem, our work emphasizes the power of CFE as a rapid prototyping platform for developing new riboswitch sensors. In a simple experiment (Figure 1B), we were able to rapidly screen eight sensor variants and immediately identify promising targets from a parallel assay. Using linear expression templates[58,59] and parallelized DNA assembly, this throughput could potentially be expanded to testing hundreds to thousands of aptamer variants at once, without even needing to assemble the full riboswitch sensor plasmids. Because there are no trans protein regulators, riboswitch sensors can be tuned in vitro just by linearly controlling the copy number of the promoter. Similarly, because our experiments monitoring matrix effects are highly modular, we expect that the workflow here could be expanded for the semi-quantitative detection of other metabolites.

Nevertheless, our study led to several key lessons learned. First, we observed that forward-designing new transcriptional riboswitches still remains more haphazard than "plug and play."[60] Although seven of the eight switches built from known aptamers responded to dopamine, only two variants had amplification ratios that would be suitable for in vitro dopamine sensing. We performed in silico analysis of the riboswitch candidates to evaluate the respective folding energies of the OFF and ON secondary structures, as well as

the predicted energetic barrier for switching configurations (Supporting Information, Table S3). However, our analyses could not identify a specific thermodynamic or kinetic parameter that explained the difference in performance between RS2 and RS8 and the remaining switches.

A second lesson learned is that converting riboswitch biosensors into useful quantitative and fieldable tests is challenging, since the sensitivity and specificity of RNA sensors is likely limiting for most clinical diagnostics. More stringent aptamer selections may be one path forward to sensitize limits of detection. However, independent of the aptamer, the weak signal that we observed when dopamine was spiked to physiological concentrations could only be detectable using electronics, and its high background signal precludes the use of enzymatic reporters that can otherwise sensitize the response.[61] We acknowledge that the estimates of matrix poisoning we develop in this work are limited to a tight operating range and to sensors with highly linear transfer functions. More work is warranted to solve inhibition from complex matrices without necessitating dilution of the target analyte.

In sum, this work serves as a proof of concept for using cell-free riboswitches for detecting human biomarkers. We anticipate that the strategies developed here will be further improved to enable on-demand rapid quantification of human health and performance biomarkers.

■ MATERIALS AND METHODS

E. coli BL21 Star (DE3) cells were purchased from Thermo Fisher (Invitrogen, Carlsbad, CA).

Phosphoenolpyruvate and *E. coli* total tRNA mixture (from strain MRE600) were purchased from Roche Applied Science (Indianapolis, IN). Dopamine hydrochloride was purchased from Tocris (Minneapolis, MN). Norepinephrine hydrochloride, serotonin hydrochloride, ampicillin, ATP, GTP, CTP, UTP, 20 amino acids, and other materials were purchased from Sigma-Aldrich (St. Louis, MO). Phusion DNA polymerase, murine RNase inhibitor, and NEBuilder HiFi DNA Assembly Master Mix were purchased from New England Biolabs (Ipswich, MA).

Plasmid Construction. All plasmids were constructed by isothermal (Gibson) assembly. Polymerase chain reaction (PCR) primers and DNA fragments were obtained from Integrated DNA Technologies (Coralville, IA). Plasmid manipulations were performed using MAX Efficiency DH5α chemically competent *E. coli* cells (Invitrogen, Carlsbad, CA). Full descriptions of primer sequences and plasmids construction techniques are available in the Supporting Information (see the Supplemental Plasmid Constructions and Supporting Information, Table S4). The sequences of all constructs have been verified by DNA sequencing (Eurofins Genomics LLC, Louisville, KY) (see Representative Riboswitch Plasmid Sequence and Representative Riboswitch Plasmid Sequence with Malachite Green Aptamer in the Supporting Information). The plasmids were purified using a QIAprep Spin Miniprep Kit (Qiagen, Valencia, CA), ethanol-precipitated, and dissolved in water.

Cell-Free Extract Preparation. Cell-free S12 extract was prepared as previously described to maximize transcription by the endogenous *E. coli* RNAP. Briefly, 1 L of 2× YT + P media (16 g/L tryptone, 10 g/L yeast extract, 5 g/L NaCl, 7 g/L potassium phosphate dibasic, 3 g/L potassium phosphate monobasic) was inoculated with 20 mL of a saturated

overnight culture of BL21 Star (DE3) in LB and grown to optical density 3.0 in 3.25 h with no induction. The cells were harvested by centrifugation at 5000g for 15 min, resuspended and washed in Buffer A (14 mM Mg-glutamate, 60 mM K-glutamate, 50 mM Tris, pH 7.7) three times, and then resuspended to a final concentration of 1 g/mL cell in Buffer A. The suspension was lysed using a QSonica Q125 sonicator with a 3.175 mm diameter probe at a frequency of 20 kHz and 50% amplitude by 10 s ON/OFF pulses until the lysed suspensions turned brown and became less viscous (around 60 s and delivering ∼ 350 J). The lysate was clarified by a 10 min centrifugation at 12,000g and 4 °C for the S12 prep. The supernatant was removed and incubated, shaking at 220 rpm for 80 min at 37 °C for the ribosomal runoff reaction. After a second 12,000g spin at 4 °C for 10 min, the supernatant from the runoff was dialyzed against Buffer B (14 mM Mg-glutamate, 60 mM K-glutamate, 5 mM Tris, pH 8.2) for 3 h at 4 °C in a 10k MWCO membrane. The dialysate was removed, centrifuged once more, aliquoted, and flash-frozen on liquid nitrogen for long-term storage at −80 °C.

Cell-Free Gene Expression Reaction. CFE reactions were prepared as previously described.[62] The overall reaction composition was 8 mM magnesium glutamate; 10 mM ammonium glutamate; 130 mM potassium glutamate; 1.2 mM ATP; 0.850 mM each of GTP, UTP, and CTP; 0.034 mg/mL folinic acid; 0.171 mg/mL yeast tRNA; 2 mM amino acids; 30 mM PEP; 0.33 mM NAD; 0.27 mM CoA; 4 mM oxalic acid; 1 mM putrescine; 1.5 mM spermidine; 57 mM HEPES; 30% S12 extract by volume; plasmid DNA to the desired concentration, and water. For matrix effect experiments, 0.2 U/μL murine RNase inhibitor was also supplied. Reactions were mixed on ice in replicates and then pipetted onto a black Corning clear-bottom 384-well plate for measurement of sfGFP (excitation/emission 485/520 nm) on a Biotek Synergy H1 plate reader either every 5 or 10 min at 30 °C. Lyophilized reactions were prepared on ice in PCR tubes with perforated caps, then immediately snap-frozen on liquid nitrogen and freeze-dried at 0.04 mbar overnight. The reactions were rehydrated with identical lyophilization volume (10 μL) with no dilution or concentration. For reactions involving human urine, frozen Pooled Human Urine (Innovative Research, Cat. IRHUURE) was thawed at 37 °C, diluted, and then added directly to the freeze-dried reactions. For reactions of the malachite green aptamer, malachite green oxalate was supplied at 10 μM, and fluorescence was measured simultaneously at excitation/emission 610/650 nm.

Statistical Analysis of Sensor Performance. Four-hour sfGFP fluorescence, normalized to a FITC calibration standard, was used for all analyses. For significance analysis in Figure 1B, a one-sided Student's *t*-test was performed for N = 3 replicates, where * indicates $p < 0.05$, ** indicates $p < 0.01$, and *** indicates $p < 0.001$. To calculate the limits of detection, we first fitted the fluorescence yields to the noncooperative logistic model

$$F = l + \frac{F_{\max} - l}{1 + \frac{K}{A}}$$

where A represents analyte concentration, l represents the sensor leak, $F_{\max}$ represents the maximum fluorescence, and K represents the half-maximal induction concentration. We then computed the LoD as the analyte concentration that would yield a fluorescence equal to $F_0 + 3 * \mathrm{STD}_0$, where F_0 is the

average fluorescence when no analyte is supplied from three technical replicates and STD_0 is the standard deviation.

RNA Structure Modeling. The secondary structure and folding energy of riboswitches were calculated using the Mfold web server (http://www.unafold.org/mfold/applications/rna-folding-form.php).[48] For all riboswitch constructs, the lowest energy conformation corresponded to the ligand-unbound OFF state with the formation of a terminator. To calculate the structure and folding energy in the ligand-bound ON state, we modeled the aptamer fold by forcing the pairing between the bases AUCACGAUUUU of the pre-aptamer sequence (see the Supporting Information) with the first 11 bases of the terminator sequence (AAAAUCCUGAU). The secondary structure of riboswitches in the OFF and ON states was transferred to the RNApathfinder[63] web server (http://bioinformatics.bc.edu/clotelab/RNApathfinder/index.spy?tab=webserver) to calculate the energy barrier that the riboswitch needed to overcome to switch into the ON state. The secondary structures in Figure 1C were rendered using VARNA.[49]

ELISA. Dopamine concentrations in spiked urine samples were determined using the DA ELISA kit (OKEH02560, Aviva Systems) according to the manufacturer's protocol. Briefly, 50 μL of serially titrated dopamine standards, diluted samples, or blank were added into wells of an anti-dopamine antibody precoated 96-well microplate, followed by immediate addition of 50 μL of 1× dopamine−biotin complex. The plate was incubated at room temperature for 60 min. After discarding the liquid in the wells, the plate was washed three times with 200 μL of 1× wash buffer, followed by addition of 100 μL of 1× avidin-horseradish peroxidase conjugate. The plate was incubated at room temperature for 45 min. After discarding the liquid and washing the plate with 3 × 200 μL of 1× wash buffer, 90 μL of 3,3′,5,5′-tetramethylbenzidine horseradish peroxidase substrate was added to each well, and the plate was incubated at 37 °C in the dark for 15−30 min until blue color was gradually developed. The enzyme reaction was stopped with 50 μL of stop solution, and yellow color development was measured at 450 nm on a microplate reader (SpectraMax Paradigm, Molecular Devices). The standard curve was generated by plotting the mean replicate relative OD_{450} of each standard serial dilution point (calculated by subtraction of mean blank well OD_{450} from well OD_{450}) vs the respective standard concentration. The concentration contained in the samples was interpolated using linear regression of each mean sample relative OD_{450} against the standard curve. The final concentration of each sample was calculated by multiplying the derived mean sample concentration by the dilution factor of 100.

ASSOCIATED CONTENT

Supporting Information

The Supporting Information is available free of charge at https://pubs.acs.org/doi/10.1021/acssynbio.1c00560.

Tables: (S1) dopamine aptamers used to design transcriptional riboswitches, (S2) reported dopamine affinity from SELEX affinity does not correlate well with cell-free activation ratio (AR), (S3) characteristics of the designed riboswitches, (S4) DNA templates used to create riboswitch constructs; Figures: (S1) dual reporter expression of dopamine riboswitch constructs, (S2) DNA titration for functional riboswitch variants, (S3) optimization of RNase inhibitor concentration and urine inhibition, (S4) filtration and boiling of urine can remove matrix effects but require auxiliary equipment, (S5) identification of the DNA concentration that provides the greatest linearity for urine matrix poisoning at saturating dopamine concentration, (S6) identification of the dopamine concentration that provides the greatest linearity for urine matrix poisoning at saturating DNA concentration, (S7) identification of the urine volume fraction concentration that provides the greatest linearity for the dopamine dose−response curve at saturating (20 nM) DNA concentration and RS2 riboswitch, (S8) ELISA and CFE calibration curves for Figure 3F, and (S9) overview of ELISA and CFE methods for dopamine quantification in urine matrix; supplemental plasmid constructions; supplemental references (PDF)

AUTHOR INFORMATION

Corresponding Author

Svetlana V. Harbaugh − 711th Human Performance Wing, Air Force Research Laboratory, Wright-Patterson Air Force Base, Ohio 45433, United States; orcid.org/0000-0001-9051-1397; Email: svetlana.harbaugh.4@us.af.mil

Authors

Adam D. Silverman − Sherlock Biosciences, Boston, Massachusetts 02135, United States

Yaroslav G. Chushak − 711th Human Performance Wing, Air Force Research Laboratory, Wright-Patterson Air Force Base, Ohio 45433, United States; Henry M. Jackson Foundation, Dayton, Ohio 45433, United States

Kathryn Zimlich − 711th Human Performance Wing, Air Force Research Laboratory, Wright-Patterson Air Force Base, Ohio 45433, United States; Henry M. Jackson Foundation, Dayton, Ohio 45433, United States

Monica Wolfe − 711th Human Performance Wing, Air Force Research Laboratory, Wright-Patterson Air Force Base, Ohio 45433, United States; UES, Inc., Dayton, Ohio 45432, United States

Walter Thavarajah − Department of Chemical and Biological Engineering, Northwestern University, Evanston, Illinois 60208, United States; Center for Synthetic Biology, Northwestern University, Evanston, Illinois 60208, United States

Michael C. Jewett − Department of Chemical and Biological Engineering, Interdisciplinary Biological Sciences Program, and International Institute of Nanotechnology, Northwestern University, Evanston, Illinois 60208, United States; Center for Synthetic Biology, Northwestern University, Evanston, Illinois 60208, United States; orcid.org/0000-0003-2948-6211

Julius B. Lucks − Department of Chemical and Biological Engineering, Interdisciplinary Biological Sciences Program, and International Institute of Nanotechnology, Northwestern University, Evanston, Illinois 60208, United States; Center for Synthetic Biology, Northwestern University, Evanston, Illinois 60208, United States; orcid.org/0000-0002-0619-6505

Jorge L. Chávez − 711th Human Performance Wing, Air Force Research Laboratory, Wright-Patterson Air Force Base, Ohio 45433, United States

2281

https://doi.org/10.1021/acssynbio.1c00560
ACS Synth. Biol. 2022, 11, 2275−2283

Complete contact information is available at:
https://pubs.acs.org/10.1021/acssynbio.1c00560

Notes

■ ACKNOWLEDGMENTS

■ REFERENCES

(1) Meyer, A.; Saaem, I.; Silverman, A.; Varaljay, V. A.; Mickol, R.; Blum, S.; Tobias, A. V.; Schwalm, N. D.; Mojadedi, W.; Onderko, E.; Bristol, C.; Liu, S.; Pratt, K.; Casini, A.; Eluere, R.; Moser, F.; Drake, C.; Gupta, M.; Kelley-Loughnane, N.; Lucks, J. P.; Akingbade, K. L.; Lux, M. P.; Glaven, S.; Crookes-Goodson, W.; Jewett, M. C.; Gordon, D. B.; Voigt, C. A. Organism Engineering for the Bioproduction of the Triaminotrinitrobenzene (TATB) Precursor Phloroglucinol (PG). *ACS Synth. Biol.* **2019**, *8*, 2746−2755.

(2) Yagur-Kroll, S.; Lalush, C.; Rosen, R.; Bachar, N.; Moskovitz, Y.; Belkin, S. Escherichia coli bioreporters for the detection of 2,4-dinitrotoluene and 2,4,6-trinitrotoluene. *Appl. Microbiol. Biotechnol.* **2014**, *98*, 885−895.

(3) Landry, B. P.; Palanki, R.; Dyulgyarov, N.; Hartsough, L. A.; Tabor, J. J. Phosphatase activity tunes two-component system sensor detection threshold. *Nat. Commun.* **2018**, *9*, No. 1433.

(4) Hua, A.; Gueuné, H.; Cregut, M.; Thouand, G.; Durand, M.-J. Development of a bacterial bioassay for atrazine and cyanuric acid detection. *Front. Microbiol.* **2015**, *6*, 211−211.

(5) Hernández-Sánchez, V.; Molina, L.; Ramos, J. L.; Segura, A. New family of biosensors for monitoring BTX in aquatic and edaphic environments. *Microb. Biotechnol.* **2016**, *9*, 858−867.

(6) Alonso, S.; Navarro-Llorens, J. M.; Tormo, A.; Perera, J. Construction of a bacterial biosensor for styrene. *J. Biotechnol.* **2003**, *102*, 301−306.

(7) Wan, X.; Volpetti, F.; Petrova, E.; French, C.; Maerkl, S. J.; Wang, B. Cascaded amplifying circuits enable ultrasensitive cellular sensors for toxic metals. *Nat. Chem. Biol.* **2019**, *15*, 540−548.

(8) Cerminati, S.; Soncini, F. C.; Checa, S. K. A sensitive whole-cell biosensor for the simultaneous detection of a broad-spectrum of toxic heavy metal ions. *Chem. Commun.* **2015**, *51*, 5917−5920.

(9) Bereza-Malcolm, L.; Aracic, S.; Franks, A. E. Development and Application of a Synthetically-Derived Lead Biosensor Construct for Use in Gram-Negative Bacteria. *Sensors* **2016**, *16*, No. 2174.

(10) Kim, H. J.; Lim, J. W.; Jeong, H.; Lee, S.-J.; Lee, D.-W.; Kim, T.; Lee, S. J. Development of a highly specific and sensitive cadmium and lead microbial biosensor using synthetic CadC-T7 genetic circuitry. *Biosens. Bioelectron.* **2016**, *79*, 701−708.

(11) Kylilis, N.; Riangrungroj, P.; Lai, H.-E.; Salema, V.; Fernández, L. Á.; Stan, G.-B. V.; Freemont, P. S.; Polizzi, K. M. Whole-Cell Biosensor with Tunable Limit of Detection Enables Low-Cost Agglutination Assays for Medical Diagnostic Applications. *ACS Sens.* **2019**, *4*, 370−378.

(12) Wu, Y.; Wang, C.-W.; Wang, D.; Wei, N. A Whole-Cell Biosensor for Point-of-Care Detection of Waterborne Bacterial Pathogens. *ACS Synth. Biol.* **2021**, *10*, 333−344.

(13) McNerney, M. P.; Michel, C. L.; Kishore, K.; Standeven, J.; Styczynski, M. P. Dynamic and tunable metabolite control for robust minimal-equipment assessment of serum zinc. *Nat. Commun.* **2019**, *10*, No. 5514.

(14) McNerney, M. P.; Piorino, F.; Michel, C. L.; Styczynski, M. P. Active Analyte Import Improves the Dynamic Range and Sensitivity of a Vitamin B12 Biosensor. *ACS Synth. Biol.* **2020**, *9*, 402−411.

(15) Thavarajah, W.; Verosloff, M. S.; Jung, J. K.; Alam, K. K.; Miller, J. D.; Jewett, M. C.; Young, S. L.; Lucks, J. B. A primer on emerging field-deployable synthetic biology tools for global water quality monitoring. *npj Clean Water* **2020**, *3*, No. 18.

(16) Slomovic, S.; Pardee, K.; Collins, J. J. Synthetic biology devices for in vitro and in vivo diagnostics. *Proc. Natl. Acad. Sci. U.S.A.* **2015**, *112*, 14429−14435.

(17) Silverman, A. D.; Karim, A. S.; Jewett, M. C. Cell-free gene expression: an expanded repertoire of applications. *Nat. Rev. Genet.* **2020**, *21*, 151−170.

(18) Silverman, A. D.; Akova, U.; Alam, K. K.; Jewett, M. C.; Lucks, J. B. Design and Optimization of a Cell-Free Atrazine Biosensor. *ACS Synth. Biol.* **2020**, *9*, 671−677.

(19) Thavarajah, W.; Silverman, A. D.; Verosloff, M. S.; Kelley-Loughnane, N.; Jewett, M. C.; Lucks, J. B. Point-of-Use Detection of Environmental Fluoride via a Cell-Free Riboswitch-Based Biosensor. *ACS Synth. Biol.* **2019**, *9*, 10−18.

(20) Liu, X.; Silverman, A. D.; Alam, K. K.; Iverson, E.; Lucks, J. B.; Jewett, M. C.; Raman, S. Design of a transcriptional biosensor for the portable, on-demand detection of cyanuric acid. *ACS Synth. Biol.* **2019**, *9*, 84−94.

(21) McNerney, M. P.; Zhang, Y.; Steppe, P.; Silverman, A. D.; Jewett, M. C.; Styczynski, M. P. Point-of-care biomarker quantification enabled by sample-specific calibration. *Sci. Adv.* **2019**, *5*, No. eaax4473.

(22) Pellinen, T.; Huovinen, T.; Karp, M. A cell-free biosensor for the detection of transcriptional inducers using firefly luciferase as a reporter. *Anal. Biochem.* **2004**, *330*, 52−57.

(23) Didovyk, A.; Tonooka, T.; Tsimring, L.; Hasty, J. Rapid and Scalable Preparation of Bacterial Lysates for Cell-Free Gene Expression. *ACS Synth. Biol.* **2017**, *6*, 2198−2208.

(24) Gräwe, A.; Dreyer, A.; Vornholt, T.; Barteczko, U.; Buchholz, L.; Drews, G.; Ho, U. L.; Jackowski, M. E.; Kracht, M.; Lüders, J.; Bleckwehl, T.; Rositzka, L.; Ruwe, M.; Wittchen, M.; Lutter, P.; Müller, K.; Kalinowski, J. A paper-based, cell-free biosensor system for the detection of heavy metals and date rape drugs. *PLoS One* **2019**, *14*, No. e0210940.

(25) Voyvodic, P. L.; Pandi, A.; Koch, M.; Conejero, I.; Valjent, E.; Courtet, P.; Renard, E.; Faulon, J.-L.; Bonnet, J. Plug-and-play metabolic transducers expand the chemical detection space of cell-free biosensors. *Nat. Commun.* **2019**, *10*, No. 1697.

(26) Jung, J. K.; Alam, K. K.; Verosloff, M. S.; Capdevila, D. A.; Desmau, M.; Clauer, P. R.; Lee, J. W.; Nguyen, P. Q.; Pastén, P. A.; Matiasek, S. J.; Gaillard, J.-F.; Giedroc, D. P.; Collins, J. J.; Lucks, J. B. Cell-free biosensors for rapid detection of water contaminants. *Nat. Biotechnol.* **2020**, *38*, 1451−1459.

(27) Pandi, A.; Grigoras, I.; Borkowski, O.; Faulon, J.-L. Optimizing Cell-Free Biosensors to Monitor Enzymatic Production. *ACS Synth. Biol.* **2019**, *8*, 1952−1957.

(28) Wen, K. Y.; Cameron, L.; Chappell, J.; Jensen, K.; Bell, D. J.; Kelwick, R.; Kopniczky, M.; Davies, J. C.; Filloux, A.; Freemont, P. S. A Cell-Free Biosensor for Detecting Quorum Sensing Molecules in *P.*

aeruginosa-Infected Respiratory Samples. *ACS Synth. Biol.* **2017**, *6*, 2293–2301.

(29) Pardee, K.; Green; Alexander, A.; Ferrante, T.; Cameron, D. E.; DaleyKeyser, A.; Yin, P.; Collins; James, J. Paper-Based Synthetic Gene Networks. *Cell* **2014**, *159*, 940–954.

(30) Pardee, K.; Green, A. A.; Takahashi, M. K.; Braff, D.; Lambert, G.; Lee, J. W.; Ferrante, T.; Ma, D.; Donghia, N.; Fan, M.; Daringer, N. M.; Bosch, I.; Dudley, D. M.; O'Connor, D. H.; Gehrke, L.; Collins, J. J. Rapid, Low-Cost Detection of Zika Virus Using Programmable Biomolecular Components. *Cell* **2016**, *165*, 1255–1266.

(31) Takahashi, M. K.; Tan, X.; Dy, A. J.; Braff, D.; Akana, R. T.; Furuta, Y.; Donghia, N.; Ananthakrishnan, A.; Collins, J. J. A low-cost paper-based synthetic biology platform for analyzing gut microbiota and host biomarkers. *Nat. Commun.* **2018**, *9*, No. 3347.

(32) Hong, F.; Ma, D.; Wu, K.; Mina, L. A.; Luiten, R. C.; Liu, Y.; Yan, H.; Green, A. A. Precise and Programmable Detection of Mutations Using Ultraspecific Riboregulators. *Cell* **2020**, *180*, 1018–1032.e16.

(33) Ma, D.; Shen, L.; Wu, K.; Diehnelt, C. W.; Green, A. A. Low-cost detection of norovirus using paper-based cell-free systems and synbody-based viral enrichment. *Synth. Biol.* **2018**, *3*, No. ysy018.

(34) Verosloff, M.; Chappell, J.; Perry, K. L.; Thompson, J. R.; Lucks, J. B. PLANT-Dx: A Molecular Diagnostic for Point-of-Use Detection of Plant Pathogens. *ACS Synth. Biol.* **2019**, *8*, 902–905.

(35) Thavarajah, W.; Silverman, A. D.; Verosloff, M. S.; Kelley-Loughnane, N.; Jewett, M. C.; Lucks, J. B. Point-of-Use Detection of Environmental Fluoride via a Cell-Free Riboswitch-Based Biosensor. *ACS Synth. Biol.* **2020**, *9*, 10–18.

(36) Porter, E. B.; Polaski, J. T.; Morck, M. M.; Batey, R. T. Recurrent RNA motifs as scaffolds for genetically encodable small-molecule biosensors. *Nat. Chem. Biol.* **2017**, *13*, 295–301.

(37) Ellington, A. D.; Szostak, J. W. In vitro selection of RNA molecules that bind specific ligands. *Nature* **1990**, *346*, 818–822.

(38) Espah Borujeni, A.; Mishler, D. M.; Wang, J.; Huso, W.; Salis, H. M. Automated physics-based design of synthetic riboswitches from diverse RNA aptamers. *Nucleic Acids Res.* **2016**, *44*, 1–13.

(39) Ceres, P.; Trausch, J. J.; Batey, R. T. Engineering modular 'ON' RNA switches using biological components. *Nucleic Acids Res.* **2013**, *41*, 10449–10461.

(40) Xiang, J. S.; Kaplan, M.; Dykstra, P.; Hinks, M.; McKeague, M.; Smolke, C. D. Massively parallel RNA device engineering in mammalian cells with RNA-Seq. *Nat. Commun.* **2019**, *10*, No. 4327.

(41) Strobel, B.; Spöring, M.; Klein, H.; Blazevic, D.; Rust, W.; Sayols, S.; Hartig, J. S.; Kreuz, S. High-throughput identification of synthetic riboswitches by barcode-free amplicon-sequencing in human cells. *Nat. Commun.* **2020**, *11*, No. 714.

(42) Findeiß, S.; Etzel, M.; Will, S.; Mörl, M.; Stadler, P. F. Design of Artificial Riboswitches as Biosensors. *Sensors* **2017**, *17*, No. 1990.

(43) Mannironi, C.; Di Nardo, A.; Fruscoloni, P.; Tocchini-Valentini, G. P. In Vitro Selection of Dopamine RNA Ligands. *Biochemistry* **1997**, *36*, 9726–9734.

(44) Lotharius, J.; Brundin, P. Pathogenesis of parkinson's disease: dopamine, vesicles and α-synuclein. *Nat. Rev. Neurosci.* **2002**, *3*, 932–942.

(45) Dalirirad, S.; Steckl, A. J. Lateral flow assay using aptamer-based sensing for on-site detection of dopamine in urine. *Anal. Biochem.* **2020**, *596*, No. 113637.

(46) Steckl, A. J.; Ray, P. Stress Biomarkers in Biological Fluids and Their Point-of-Use Detection. *ACS Sens.* **2018**, *3*, 2025–2044.

(47) Perry, M.; Li, Q.; Kennedy, R. T. Review of recent advances in analytical techniques for the determination of neurotransmitters. *Anal. Chim. Acta* **2009**, *653*, 1–22.

(48) Zuker, M. Mfold web server for nucleic acid folding and hybridization prediction. *Nucleic Acids Res.* **2003**, *31*, 3406–3415.

(49) Darty, K.; Denise, A.; Ponty, Y. VARNA: Interactive drawing and editing of the RNA secondary structure. *Bioinformatics* **2009**, *25*, 1974–1975.

(50) Chushak, Y.; Harbaugh, S.; Zimlich, K.; Alfred, B.; Chávez, J.; Kelley-Loughnane, N. Characterization of synthetic riboswitch in cell-free protein expression systems. *RNA Biol.* **2021**, *18*, 1727–1738.

(51) Siegal-Gaskins, D.; Tuza, Z. A.; Kim, J.; Noireaux, V.; Murray, R. M. Gene Circuit Performance Characterization and Resource Usage in a Cell-Free "Breadboard". *ACS Synth. Biol.* **2014**, *3*, 416–425.

(52) Nshogozabahizi, J. C.; Aubrey, K. L.; Ross, J. A.; Thakor, N. Applications and limitations of regulatory RNA elements in synthetic biology and biotechnology. *J. Appl. Microbiol.* **2019**, *127*, 968–984.

(53) Breaker, R. R. Riboswitches and the RNA world. *Cold Spring Harbor Perspect. Biol.* **2012**, *4*, No. a003566.

(54) Naccarato, A.; Gionfriddo, E.; Sindona, G.; Tagarelli, A. Development of a simple and rapid solid phase microextraction-gas chromatography–triple quadrupole mass spectrometry method for the analysis of dopamine, serotonin and norepinephrine in human urine. *Anal. Chim. Acta* **2014**, *810*, 17–24.

(55) Soltani, M.; Hunt, J. P.; Bundy, B. C. Rapid RNase inhibitor production to enable low-cost, on-demand cell-free protein synthesis biosensor use in human body fluids. *Biotechnol. Bioeng.* **2021**, *118*, 3973–3983.

(56) Voyvodic, P. L.; Conejero, I.; Mesmoudi, K.; Renard, E.; Courtet, P.; Cattoni, D. I.; Bonnet, J. Evaluating and Mitigating Clinical Samples Matrix Effects on TX-TL Cell-Free Performance. *bioRxiv* **2022**, No. 489947.

(57) Inan, H.; Öztekin, E. Phosphate and nitrogen removal by iron produced in electrocoagulation reactor. *Desalin. Water Treat.* **2014**, *52*, No. 1396.

(58) Sun, Z. Z.; Yeung, E.; Hayes, C. A.; Noireaux, V.; Murray, R. M. Linear DNA for Rapid Prototyping of Synthetic Biological Circuits in an Escherichia coli Based TX-TL Cell-Free System. *ACS Synth. Biol.* **2014**, *3*, 387–397.

(59) Michel-Reydellet, N.; Woodrow, K.; Swartz, J. Increasing PCR Fragment Stability and Protein Yields in a Cell-Free System with Genetically Modified *Escherichia coli* Extracts. *J. Mol. Microbiol. Biotechnol.* **2005**, *9*, 26–34.

(60) Etzel, M.; Mörl, M. Synthetic Riboswitches: From Plug and Pray toward Plug and Play. *Biochemistry* **2017**, *56*, 1181–1198.

(61) Lopreside, A.; Wan, X.; Michelini, E.; Roda, A.; Wang, B. Comprehensive Profiling of Diverse Genetic Reporters with Application to Whole-Cell and Cell-Free Biosensors. *Anal. Chem.* **2019**, *91*, 15284–15292.

(62) Silverman, A. D.; Kelley-Loughnane, N.; Lucks, J. B.; Jewett, M. C. Deconstructing Cell-Free Extract Preparation for in Vitro Activation of Transcriptional Genetic Circuitry. *ACS Synth. Biol.* **2019**, *8*, 403–414.

(63) Dotu, I.; Lorenz, W. A.; Van Hentenryck, P.; Clote, P. Computing folding pathways between RNA secondary structures. *Nucleic Acids Res.* **2010**, *38*, 1711–1722.